

# Synthesis and Characterization of Poly(methyl methacrylate)-*g*-poly(dimethylsiloxane) Copolymers. 1. Bulk and Surface Characterization

S. D. Smith,<sup>†</sup> J. M. DeSimone,<sup>‡</sup> H. Huang,<sup>§</sup> G. York,<sup>⊥</sup> D. W. Dwight,<sup>||</sup> G. L. Wilkes, and J. E. McGrath\*

Departments of Chemistry and Chemical Engineering, NSF Science and Technology Center: High Performance Polymeric Adhesives and Composites, Virginia Polytechnic Institute and State University, Blacksburg, Virginia 24061

Received January 17, 1991; Revised Manuscript Received December 17, 1991

**ABSTRACT:** Poly(methyl methacrylate)-*g*-poly(dimethylsiloxane) copolymers were prepared using the macromonomer technique. Poly(dimethylsiloxane) (PDMS) macromonomers of controlled molar masses, narrow molar mass distributions, and high percent functionalities were synthesized through the utilization of the living anionic ring-opening polymerization of hexamethylcyclotrisiloxane. The resultant methacryloxy-functionalized macromonomers, having a range of molar masses, were statistically copolymerized with methyl methacrylate to form the title graft copolymers of various chemical compositions. The bulk phase morphology of the well-defined graft copolymers was investigated using DSC, DMTA, DMA (Rheovibron), TEM, and SAXS. Surface segregation of the low surface energy component, PDMS, was established using angular-dependent X-ray photoelectron spectroscopy and advancing water contact angle measurements. The thorough characterization of this heterophase polymeric system allowed the elucidation of the relationship between the polymer architecture and the bulk and surface properties of the system.

## Introduction

Multiphase polymeric systems are an important class of materials that have the ability to exhibit the physical properties of both components. The capacity to synthesize materials of this type is varied.<sup>1</sup> The traditional methodologies that are available to synthesize heterophase materials include step-growth polymerization processes,<sup>2</sup> living anionic<sup>3,4</sup> and cationic chain-growth systems,<sup>5</sup> traditional "grafting from" free-radical methods,<sup>6</sup> and finally the macromonomer technique established by Rempp<sup>7</sup> and Milkovich.<sup>8</sup>

Living polymerization methods allow the synthesis of polymers of controlled molar mass having a narrow molar mass distribution. Of particular interest to this study was poly(dimethylsiloxane) (PDMS) macromonomers synthesized through the anionic organolithium-initiated ring-opening polymerization of hexamethylcyclotrisiloxane (D<sub>3</sub>). This investigation involved the functional termination of the living polymerization with a chlorosilane derivative of allyl methacrylate to afford a methacryloxy-functionalized PDMS macromonomer which was subsequently statistically copolymerized with MMA to afford the title graft copolymers.

The incorporation of microphase-separated PDMS domains into a PMMA matrix allows the system to exhibit many of the often desirable properties of both components. The PMMA matrix is known to possess very good optical clarity, good UV stability, high electrical resistivity, and

hydrolytic stability. Some of the desirable properties of PDMS include a very low glass transition temperature, biocompatibility, low surface energy, high oxygen permeability, and resistance toward degradation by atomic oxygen and oxygen plasmas. A heterophase material therefore, consisting of microphase-separated PDMS domains embedded in a PMMA matrix, such as the graft copolymers synthesized in this paper, should illustrate the desirable properties of both components. The synthesis, bulk phase morphology, and surface properties of the PMMA-*g*-PDMS system will be presented below.

## Experimental Section

**Reagents.** Cyclohexane (Fisher, Reagent Grade) was stirred over concentrated sulfuric acid for ca. 2 weeks, decanted, and distilled under nitrogen from a sodium dispersion. Tetrahydrofuran (Fisher, Certified Grade) was distilled under nitrogen from the purple sodium/benzophenone ketyl. Toluene (Fisher) was thoroughly degassed and used directly in free-radical polymerization. Hexamethylcyclotrisiloxane (D<sub>3</sub>) was generously provided by General Electric. The cyclic monomer was melted, stirred over finely divided calcium hydride for ca. 12 h, and sublimed under vacuum. The sublimed monomer was then dissolved in purified cyclohexane to obtain stock solutions of ca. 50% (w/v) solids and stored under nitrogen. Methyl methacrylate (MMA) (Rohm and Haas) was vacuum distilled from finely divided calcium hydride and stored at -20 °C under nitrogen.

**Macromonomer Synthesis.** Anionic polymerizations were carried out in rigorously cleaned and dried one-neck round-bottom flasks equipped with a magnetic stirrer and rubber septum under a 6-8-psig prepurified nitrogen atmosphere. The cyclohexane solution of D<sub>3</sub> was syringed into the reaction flask, and a calculated amount of *sec*-butyllithium was added to initiate the ring-opening polymerization. The initiation reaction was allowed to proceed for ca. 2 h, followed by the addition of ca. 10% by volume THF to promote propagation of the living siloxanolate species. The polymerization was terminated with [3-(methacryloxy)propyl]-dimethylchlorosilane (MPDC) (Petrarch) to afford the macromonomer, which was then precipitated in methanol and dried under reduced pressure at room temperature. The PDMS macromonomers were characterized by ultraviolet spectroscopy (Perkin-Elmer Model 552), <sup>1</sup>H NMR (Bruker WP 270), vapor phase

\* To whom correspondence should be addressed.

<sup>†</sup> Current address: Procter and Gamble Co., Miami Valley Laboratory, Cincinnati, OH 45239-8707.

<sup>‡</sup> Current address: Department of Chemistry, University of North Carolina at Chapel Hill, C.B. 3290, Venable and Kenan Laboratories, Chapel Hill, NC 27599-3290.

<sup>§</sup> Current address: BOC Group Technical Center, 100 Mountain Ave., Murray Hill, NJ 07974.

<sup>⊥</sup> Current address: Shell Development Co., Westhollow Research Center, P.O. Box 1380, Houston, TX 77251-1380.

<sup>||</sup> Current address: Department of Chemistry, Lehigh University, Bethlehem, PA 18015.

osmometry (Wescan), and GPC (Waters 590 GPC with Ultrastaygel columns of 500-, 10<sup>3</sup>-, 10<sup>4</sup>-, 10<sup>5</sup>-, and 10<sup>6</sup>-Å porosities in toluene) using poly(dimethylsiloxane) standards, to confirm not only their molar mass and molar mass distribution but also their end-group functionality.

**Free-Radical Copolymerization.** The free-radical copolymerizations of the PDMS macromonomer with MMA were performed in degassed toluene at 65 °C for ca. 50 h using 0.1 wt % (based on MMA) azobis(isobutyronitrile) (Vazo 64). The copolymerization were carried out at 20 wt % solids under a 6–8-psig nitrogen atmosphere. The graft copolymers were precipitated in methanol and dried under reduced pressure, followed by extensive extraction with hexanes to remove any unreacted PDMS macromonomer. Under appropriate conditions, the copolymerizations resulted in conversions of ca. 100% of the MMA and ca. 80–90% of the macromonomer.

**Copolymer Characterization.** The graft copolymers were characterized by a number of techniques. The compositions were determined using  $^1\text{H}$  NMR spectroscopy (Bruker WP 270). The molar masses and molar mass distributions were investigated using membrane osmometry (Wescan Model 231 recording membrane osmometer) and size exclusion chromatography with refractive index, ultraviolet, and differential viscometric detectors (Waters 150-C GPC with 500-,  $10^3$ -,  $10^4$ -,  $10^5$ -, and  $10^6$ -Å porosities in THF, with a Viscotek Model 100 differential viscometric detector).

Differential scanning calorimeter (DSC) thermograms were obtained on a Perkin-Elmer DSC-2 run at  $10^{\circ}\text{C min}^{-1}$ . Dynamic mechanical analysis (DMA) was carried out by a DDV-IIC Rheovibron dynamic viscoelastometer in conjunction with an automation system from Imass Inc. The heating rate was controlled at  $1\text{--}2^{\circ}\text{C min}^{-1}$  and the operating frequency was 11 Hz. All of the samples for this experiment were first annealed at  $140^{\circ}\text{C}$  for 14 hours and then slowly cooled to room temperature to minimize any residual trace of solvent.

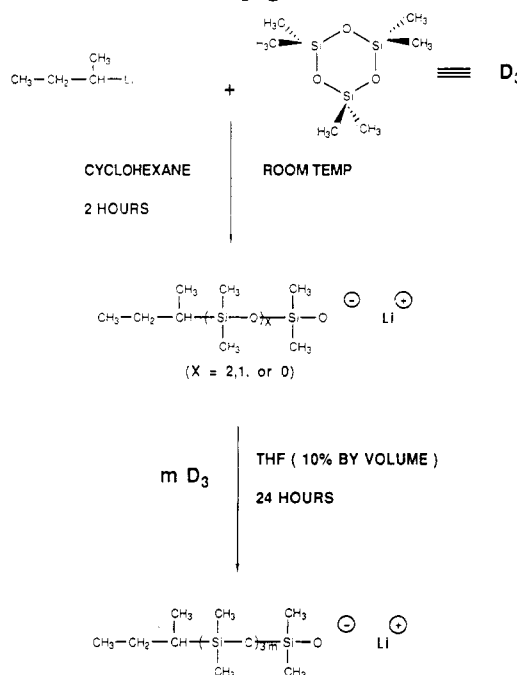
Samples for SAXS and TEM were prepared by slow evaporation (ca. 48 h) of dilute chloroform solutions of the copolymers. TEM specimens were ultracryomicrotomed from these films. ESCA samples were prepared by slow evaporation of chloroform solutions onto metal plates of the appropriate size. All films were dried under vacuum at 25 °C for 12 h. Small-angle X-ray scattering (SAXS) was carried out using a Siemens Kratky camera system with a copper target X-ray source. The entrance slit was 30  $\mu\text{m}$ , and the operating conditions were 40 kV and 20 mA. A position-sensitive detector system (PSD) from M. Braun Inc. was used. A computer program written by Vonk and co-workers was utilized for obtaining the correlation function and the invariant. ESCA was carried out on a Kratos XSAM-800 instrument with a Mg anode, 200 W at a vacuum of  $10^{-9}$  Torr. TEM analysis was done on a Philips EM 420 STEM at 100 kV in the TEM mode.

## Results and Discussion

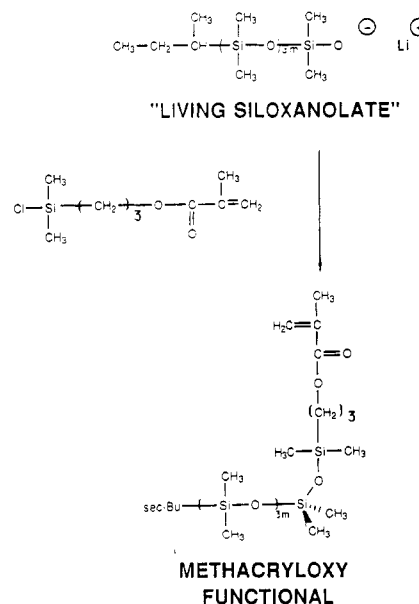
The macromonomer technique has received considerable attention in recent years.<sup>9-11</sup> However, poly(dimethylsiloxane) (PDMS) "macromonomers" were reported by Greber<sup>12</sup> in 1962. In our work, copolymerizations with various alkyl methacrylates, including methyl methacrylate, were carried out in which the number-average molar mass of the PDMS macromonomer was varied from 1000 to 20 000 g/mol and the composition of the copolymer was varied from 5 to 60% (w/w) PDMS.<sup>13-19</sup>

The preparation of methacryloxy-functionalized poly-(dimethylsiloxane)<sup>20,21</sup> macromonomers of high functionality, illustrated in Schemes I and II, was an important first step in the preparation of the well-defined graft copolymers. The addition of *sec*-butyllithium to the pure cyclohexane solution of D<sub>3</sub> results in the initiation of the ring-opening polymerization without any further propagation. The reason for this is that in nonpolar solvents, such as cyclohexane, the living siloxanolate exists as a very tight ion pair with the lithium counterion. Upon the addition of the polar solvent, THF, the polarity of the

**Scheme I**  
**Synthesis of PDMS Macromonomers: Initiation and Propagation**



**Scheme II**  
**Synthesis of PDMS Macromonomers: Functional Termination**



solution changes, which loosens the ion pair, allowing propagation to occur to afford high polymer of controlled molar mass in a living manner.<sup>22-25</sup> The polymerization was functionally terminated with MPDC. The number-average molar mass of the PDMS macromonomers was characterized by VPO. The end-group functionality and the molar mass were determined by end-group analysis using proton NMR and UV spectroscopy. UV analysis was performed at 214 nm in THF (Figure 1), allowing the detection of the ester carbonyl of the methacryloxy functional end group. As can be seen in Table I, a good correspondence between the NMR and UV results was obtained. Another check on the functionality of the PDMS macromonomers was their incorporation into copolymers under free-radical conditions. Proton NMR was used to confirm the amount of PDMS incorporation into the copolymers (Table II). It was observed that the incor-

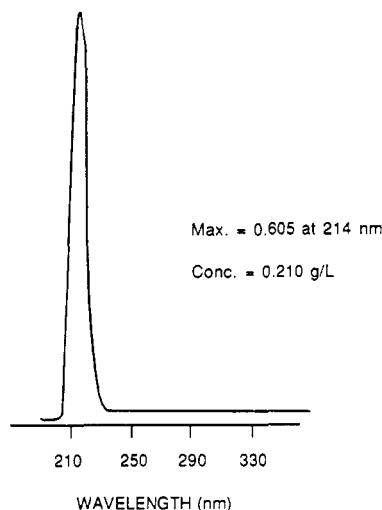


**Figure 1.** UV spectrum of methacryloxy-functionalized PDMS macromonomer with  $\bar{M}_n = 1600$  g/mol.

**Table I**  
 $\bar{M}_n$  Values (g/mol) of Methacrylate Functional Poly(dimethylsiloxane) via Spectroscopic and Osmotic Techniques

sample	theor	$^1\text{H NMR}^a$	VPO <sup>b</sup>	UV <sup>c</sup>
1	5000		6500	6000
2	1500	1600	1500	1700
3	1000	900	1030	900

<sup>a</sup> Comparison of silicon methyl/methacrylate methyl. <sup>b</sup> Solvent: toluene. <sup>c</sup> From ester carbonyl absorbance at 214 nm (UV).

**Table II**  
Synthesis of PMMA-*g*-PDMS

PDMS/macromonomer $\bar{M}_n$ , g/mol	wt % PDMS charged	wt % PDMS incorp via NMR
1000	5	4
	10	8
	15	9
	20	15
5000	5	4
	10	7
	15	12
	20	17
10000	5	6
	10	10
	15	14
	20	16
20000	5	4
	10	7
	20	12

porated amounts of PDMS macromonomer are relatively close to the charged amounts, indicating high functionality. It is important to note that the concentration of the copolymerization reaction was maintained at 20% (w/v). This was determined to be an adequate concentration upon which macrophase separation did not occur during the copolymerization. This undesirable phenomenon easily occurs at higher concentrations, especially with the highest molar mass macromonomers.

Calculations on the number of grafts per backbone were conducted to estimate the average number of grafts per given chain length and composition. Table III summarizes the calculations for a chain with a molar mass of 100 000 g/mol for varying graft molar masses and compositions. Several important conclusions can be drawn from this table. For example, at any given composition a wide range of chain topologies (architectures) is possible. Also, at high graft molar mass and low graft content it is likely

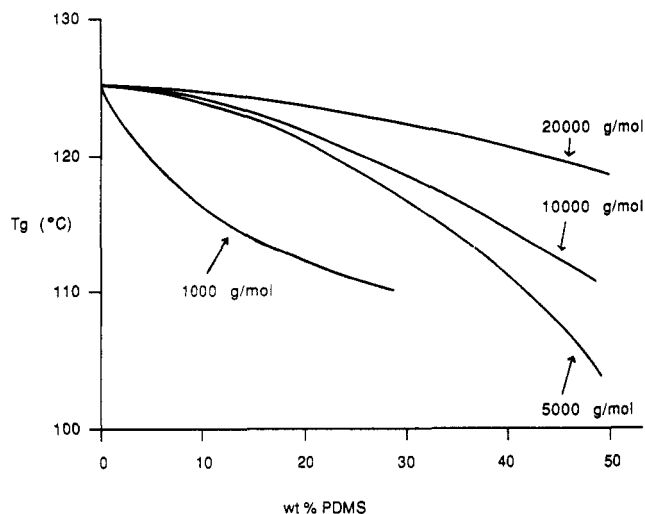


**Figure 2.** Upper glass transition temperatures of PMMA-*g*-PDMS as a function of PDMS graft molar mass and weight percent PDMS.

**Table III**  
Calculated Number of Branches per Copolymer Molecule of Total  $\bar{M}_n = 100\,000$  g/mol

graft $\bar{M}_n$	wt % PDMS graft				
	10	20	30	40	50
1000	10	20	30	40	50
5000	2	4	6	8	10
10000	1	2	3	4	5

that there is fewer than one graft per chain. This is especially important to consider for copolymers of molar mass less than 100 000 g/mol, since with decreasing degree of polymerization there will be fewer grafts per chain. Complementary studies have focused on fractionation and chemical composition distribution studies, which have further elucidated these points.<sup>26,27</sup> All of these observations indicate that the structural variables present in graft copolymers prepared by the macromonomer method are more numerous than for block copolymers and that these parameters will inevitably play a role in the structure/property relationships.

The PDMS graft molar mass and copolymer compositions dictate the properties of the system, as was evidenced by several techniques. From DSC measurements, phase mixing is indicated for copolymers containing low molar mass grafts, as evidenced by a shifting of the  $T_g$  of PMMA to lower temperatures (Figure 2). The  $T_g$ 's of copolymers with graft molar masses of 5000, 10 000, and 20 000 are roughly equivalent at low siloxane levels; however, changes in the breadths of the transitions indicate differences in phase mixing, which is to be expected. As can be seen in Figure 2, increasing the siloxane content of the graft copolymers causes the upper  $T_g$ 's of copolymers to fall, indicating partial miscibility for even the higher molar mass grafts. Similar results are observed by DMA and will be discussed later. The results are summarized in Table IV.

Low-temperature transitions were also measured by DSC and are summarized in Table V. Materials with low siloxane content show weak glass transitions and no evidence of PDMS crystallization or melting. At higher siloxane contents, however,  $T_c$ 's and  $T_m$ 's are observed. Comparison of the transitions in the copolymers to PDMS homopolymers of similar molar masses indicates partial miscibility of the PMMA into the PDMS phase. The absence of a low-temperature transition by DSC in the 5000 g/mol and lower graft systems further indicates

**Table IV**  
Influence of Graft Molar Mass on Glass Transition Temperature ( $T_g$ , °C) for PMMA-*g*-PDMS Copolymers (~16 wt % PDMS)

macromonomer $\bar{M}_n$	PMMA $T_g$		
	by DSC	by DMTA (1 Hz)	by DMA (11 Hz)
1000	111	110	138
5000	123	123	142
10000	125	126	
20000	127		146
pure PMMA <sup>a</sup>	132	132	148

<sup>a</sup> Syndiotactic PMMA prepared anionically.

**Table V**  
Glass Transition Temperatures of Some PMMA-*g*-PDMS Copolymers

graft $\bar{M}_n$ , g/mol	wt % PDMS	$T_g$ , °C	$T_c$ , °C	$T_m$ , °C
1000	20	-112		
5000	20	-110		
10000	20	-113		
20000	20	-126		
5000	45	-126		
10000	45	-127	-101	-55
20000	45	-123	-111	-45

substantial mixing of the phases.

To obtain further evidence on the degree of phase separation, dynamic mechanical experiments were carried out, and the results of the  $\tan \delta$  behavior for these materials are shown in Figure 3. Also shown as a reference in this figure is a  $\tan \delta$  spectrum for a pure PMMA sample. The temperature at which the maximum in  $\tan \delta$  occurred was taken as the glass transition temperature, and the values are listed in Table IV. For the case of the highest molar mass PDMS graft (20 000 g/mol), the low-temperature transition was distinct.

Also, the  $T_g$  for the PMMA phase is rather close to that of the control pure PMMA material. This suggests that the mixing is low and what occurs most likely takes place only in the interfacial region.<sup>28</sup> As the PDMS molar mass decreases to 5000 g/mol, the PDMS  $T_g$  shifts to a slightly higher temperature while the PMMA  $T_g$  becomes lower. Again, this indicates further mixing but may represent principally mixing in the interfacial region. From the absence of a siloxane melting peak in the  $\tan \delta$  spectra one could conclude that *the microphase separation apparently is not very sharp, thereby depressing the crystallization*. For the system with PDMS molar mass of 1000 g/mol, significant differences are observed relative to the other materials. First, the low-temperature PDMS transition is no longer significant but a broad dispersion is observed in the temperature range from -100 to -70 °C. Furthermore, the PMMA  $T_g$  shifts 10 °C from that of the pure PMMA. Both of these observations suggest that the degree of mixing extends beyond the interphase region.<sup>28</sup> This postulation is also consistent with the SAXS results which will be presented later.

The SAXS profiles of a series of solvent (chloroform)-cast PMMA-*g*-PDMS samples having 16 wt % PDMS of various molar masses are shown in Figure 4. The variable  $s$  is defined as  $(2 \sin \theta)/\lambda$ , where  $\theta$  is half the scattering angle and  $\lambda$  is the wavelength. A maximum is observed in each sample, indicating the existence of a correlation distance which should correspond to the average spacing between siloxane domains. As the PDMS molar mass increases, the value of  $s$  at which the maximum occurs decreases, suggesting an increase in the interdomain spacing. To further quantify this information, a corre-

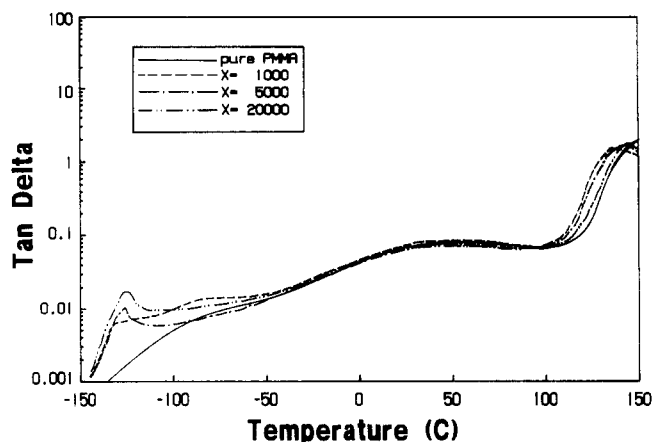


Figure 3. DMTA  $\tan \delta$  response for the 16 wt % PDMS system.

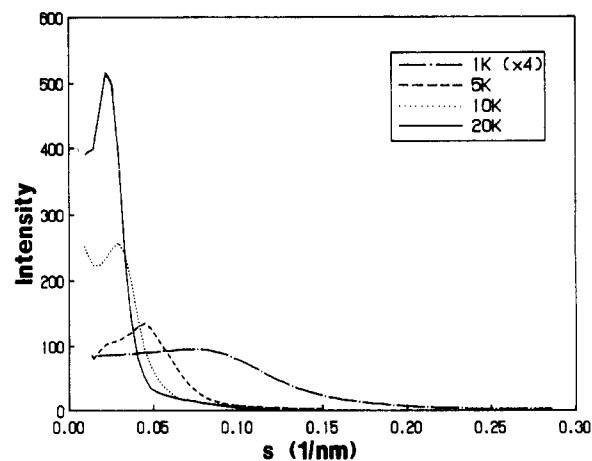


Figure 4. Small-angle X-ray scattering profiles for chloroform-cast PMMA-*g*-PDMS films having 16 wt % PDMS and variable PDMS graft molar mass.

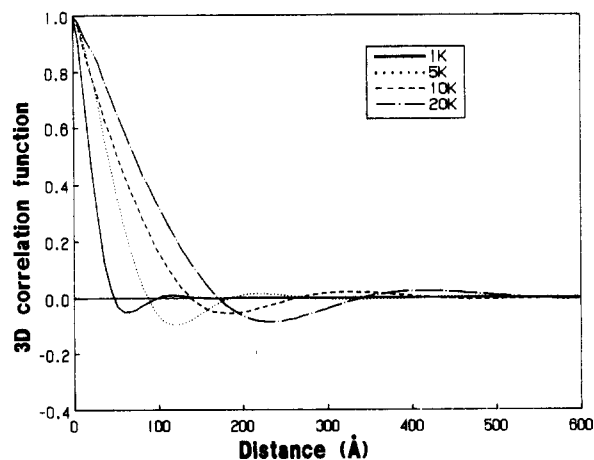


Figure 5. Corresponding SAXS correlation function results.

lation function for each sample was calculated, and the results are shown in Figure 5. The magnitude of  $r$  at the first maximum of this 3-D correlation function is commonly known as the correlation length, which is an estimation of the interdomain spacing. For the present systems, these spacings from the SAXS results are listed in column 2 of Table VI. As suggested above, this value increases with the PDMS molecular weight. Since the volume fraction of PDMS is approximately the same for these samples, this increasing interdomain spacing suggests an increase in the domain size.

For a dilute particulate scattering system, another important article of information that can be deduced from

**Table VI**  
SAXS Analysis of PMMA-*g*-PDMS Copolymer with 16 wt % PDMS

PSX $M_n$ , g/mol	interdomain spacing, Å		domain size, Å		$(\Delta\rho)^2 \times 10^3$ , (mol e/cm <sup>3</sup> ) <sup>2</sup>	deg of separation, %
	SAXS	TEM	SAXS	TEM		
1000	115		40		0.908	35
5000	220	157	75	80	1.183	46
10000	324	210	109	150	1.264	49
20000	411	316	142	200	1.380	53

the SAXS correlation function is the coherence length,  $l_c$ , which is an estimation of the particle size. For the present systems, it may be used to approximate the size of the PDMS domains. By definition the coherence length, which can be viewed as a weight average of the particle size,<sup>29</sup> is calculated as follows:

$$l_c = 2 \int_0^\infty \gamma(r) dr = l^2 / \bar{l}$$

where  $\gamma(r)$  is the correlation function and  $l$  is the particle size or, in this case, the domain size. One point to note is that although  $l_c$  is developed for dilute systems (that is to say where the interference term between particles is negligible), it is relatively insensitive to the density of the packing.<sup>29</sup> Therefore, it should still provide an estimation of the domain size, although it is not expected to directly match with those obtained from the TEM analysis.

Following the above reasoning, the PDMS domain sizes in the systems under investigation were estimated by calculating  $l_c$  from the correlation functions, shown in Figure 5. The results are shown in column 4 of Table VI. As expected from the increasing interdomain spacing, the domain size increases with PDMS molar mass.

In addition to the interdomain spacing and domain size, SAXS results can also offer information about the degree of phase separation through an invariant analysis. In principle, the X-ray scattering technique is based on the contrast resulting from the variation in electron density. Sharper phase separation will result in higher contrast and, hence, a higher magnitude of electron density fluctuation. For the extreme case of a two-phase system with sharp boundaries and no mixing, the mean square electron density fluctuation  $(\Delta\rho)^2$  is well-known to be<sup>29</sup>

$$(\Delta\rho)^2 = \phi_a \phi_b (\rho_a - \rho_b)^2$$

where  $\rho_a$  and  $\rho_b$  are the electron densities of the two components, respectively. By normalizing  $(\Delta\rho)^2$  of a specific system with respect to this extreme case, a value between 0 and 1 can be obtained which may be used as an index for the degree of phase separation.

For the present system, the mean square electron density fluctuations were calculated from the SAXS profiles, and the values are listed in column 6 of Table VI. An increasing trend with PDMS molar mass is observed. Since the volume fraction of the siloxane component is approximately the same for all four materials, this increasing trend indicates an increasing degree of phase separation. To further quantify this,  $(\Delta\rho)^2$  for each sample was normalized with respect to the extreme case of a "sharp phase boundary" (which was calculated to be 2.6 (mol e/cm<sup>3</sup>)<sup>2</sup>), and the results are listed in the last column of Table VI. The increasing trend in degree of separation with PDMS molar mass is consistent with the DSC results shown earlier and the DMA results discussed later in this paper. Also, one notes that the level of separation is considerably lower in the system with the lowest PDMS molar mass graft, as would be expected. This low value suggests a rather high degree of mixing taking place between the two block

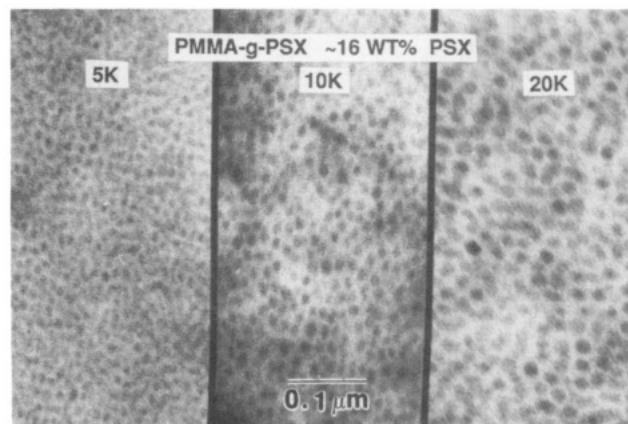


**Figure 6.** Transmission electron micrographs of chloroform-cast PMMA-*g*-PDMS having 16 wt % PDMS and 5000, 10 000, and 20 000 g/mol PDMS grafts.

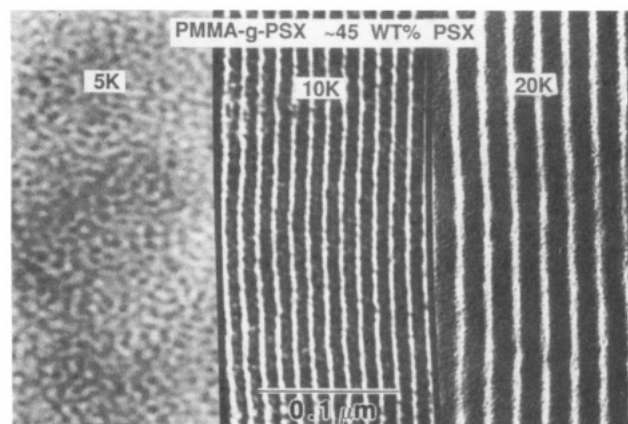


**Figure 7.** Transmission electron micrographs of chloroform-cast PMMA-*g*-PDMS having 45 wt % PDMS and 5000, 10 000, and 20 000 g/mol PDMS grafts.

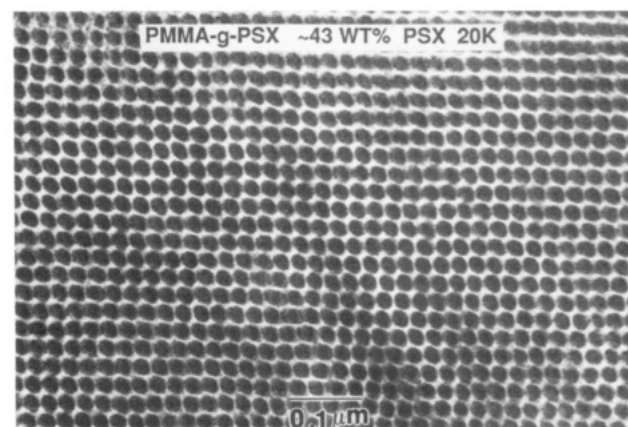


**Figure 8.** Transmission electron micrograph of the PMMA-*g*-PDMS copolymer having 43 wt % PDMS with 20 000 g/mol PDMS grafts showing an end-on view of the cylindrical morphology.

components. This is consistent with the significant  $T_g$  depression of the PMMA. One point to emphasize is that the level of separation should only be viewed as an *index for relative comparison*; any further interpretation on the absolute values may be questionable. Clearly, the SAXS results are very supportive of the data reported earlier.

From transmission electron microscopy (TEM), the morphology of the poly(methyl methacrylate) graft systems changed significantly as a function of architecture and composition (Figures 6–8). Specifically, at the lower PDMS contents, the morphology was a spherical domain

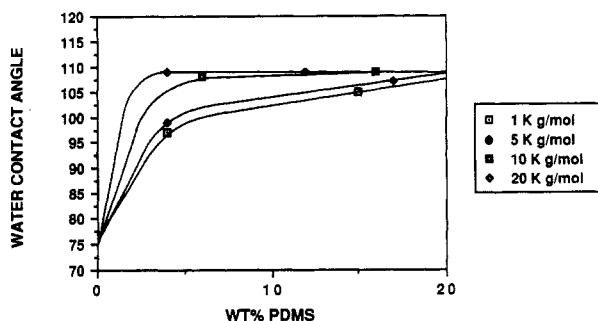


**Figure 9.** Advancing water contact angle measurements of the PMMA-*g*-PDMS system as a function of composition and PDMS graft molar mass.

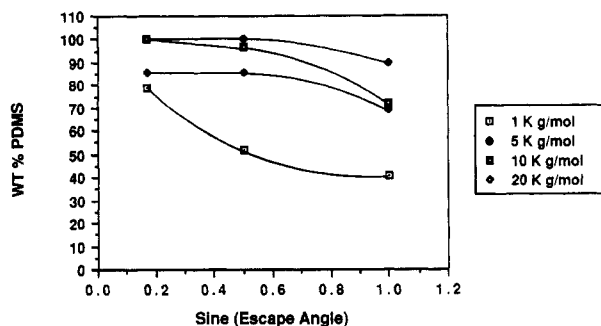


**Figure 10.** Angular-dependent X-ray photoelectron spectroscopy results plotted as a function of weight percent PDMS and sin (sampling angle).

texture but changed to a ordered cylindrical texture when the PDMS content was 45 wt %. The average domain sizes vary from 80 Å for the 5000 g/mol grafts to 200 Å for the 20 000 g/mol grafts, while the 1000 g/mol graft systems showed no apparent phase separation. The lack of observation of PDMS domains for the graft polymer having 1000 g/mol grafts is consistent with the DSC results which showed a significant  $T_g$  depression for the PMMA. For comparison, the interdomain spacings and the domain sizes measured from TEM micrographs are also listed in Table VI (column 3). There is some discrepancy in the values observed by SAXS and TEM, but the trend from both techniques is consistent. The lower values of domain spacing by TEM relative to the values obtained from SAXS can be related to the inherent problem of projecting a three-dimensional object on a two-dimensional surface; however, the relative trends are valid and useful for interpretation.

Since poly(dimethylsiloxane) has a low surface energy and it exists in a microphase-separated system, we would expect it to dominate the air/solid or vacuum/solid interface in these copolymers.<sup>30</sup> Water contact angle measurements indeed indicated a change in surface composition with molar mass and composition of the grafts. Copolymers containing higher molar mass grafts, which exhibit a higher degree of phase separation, have higher contact angles, probably due to the presence of a more complete layer of the PDMS at the surface (Figure 9). This agrees with several results from our laboratory and elsewhere.<sup>18,19</sup> Again the 1000 g/mol graft system does not dominate the surface at low siloxane compositions, indicating surface mixing.

X-ray photoelectron spectroscopy (XPS) was used as a tool to quantify the surface composition. Angular-dependent XPS depth profiling demonstrated that the surface had a gradient of composition and that the surface was observed to be of higher PDMS concentration for higher molar mass PDMS grafts. It is noteworthy to say that

higher angles penetrate deeper into the surface and as an approximation, an angle of 10° measures about the top 10 Å of the surface, while an angle of 30° looks at about the top 15 Å, and finally the 90° measurement indicates the composition down to about 60 Å. Figure 10 shows these data plotted as percent PDMS versus sampling angle. Clearly, important trends in composition with graft molar mass and depth are observed. It is evident that two different situations are present. In copolymers with well phase separated bulk morphologies, there probably exists a relatively thick surface layer of siloxane, and the curves for these materials as a function of angle are relatively flat. Conversely, in materials with a significant amount of phase mixing, only a thin layer of siloxane exists, and the curves for these materials show an exponential type decay in siloxane content with depth into the surface.

## Conclusions

Methacryloxy-functionalized PDMS macromonomers were successfully synthesized using living polymerization techniques. These PDMS macromonomers were efficiently copolymerized with MMA under free-radical conditions to afford PMMA-*g*-PDMS copolymers. The SAXS results show that a correlation length exists in each sample, and this length should correspond to the interdomain spacing of the siloxane phases. The SAXS and TEM results both indicate that as the graft molar mass increases, both the size and the interdomain spacing increase. Furthermore, from the invariant analysis, the degree of phase separation becomes greater with increasing PDMS molar mass. This conclusion was also supported by the dynamic mechanical and DSC data.

**Acknowledgment.** Support by the NSF Center on High Performance Polymeric Adhesives and Composites under Contract DMR-8809714 is appreciated.

## References and Notes

- (1) Noshay, A.; McGrath, J. E. *Block Copolymers: Overview and Critical Survey*; Academic Press: New York, 1977.
- (2) Riess, G.; Hurtrez, G.; Bahador, P. *Block Copolymers*. In *Encyclopedia of Polymer Science and Engineering*, 2nd ed.; Kroschwitz, J., Ed.; Wiley: New York, 1985; Vol. 2, pp 324-434.
- (3) Zelinski, R. P.; Childers, C. W. *Rubber Chem. Technol.* **1968**, *41*, 161.
- (4) Schlick, S.; Levy, M. *J. Phys. Chem.* **1960**, *64*, 883.
- (5) Higashimura, T.; et al. *Makromol. Chem., Macromol. Symp.* **3** **1986**, *83*, 99.
- (6) Brydon, A.; Burnett, G.; Cameron, G. G. *J. Polym. Sci., Polym. Chem. Ed.* **1973**, *11* (12), 3255.
- (7) Rempp, P.; Lutz, P.; Masson, P.; Franta, E. *Makromol. Chem.* **1984**, *8*, 3.
- (8) Schulz, G. O.; Milkovich, R. *J. Appl. Polym. Sci.* **1982**, *27*, 4773.
- (9) Rempp, P.; Lutz, P.; Masson, P.; Franta, E. *Makromol. Chem., Suppl.* **1984**, *8*, 3.
- (10) Rempp, P.; Franta, E. *Adv. Polym. Sci.* **1984**, *58*.
- (11) Yamashita, Y. *J. Polym. Sci.* **1981**, *36*, 193.
- (12) Greber, G.; Reese, E. *Makromol. Chem.* **1962**, *55*, 96.
- (13) Smith, S. D.; McGrath, J. E. *Polym. Prepr. (Am. Chem. Soc., Div. Polym. Chem.)* **1986**, *27* (2), 31.
- (14) Smith, S. D.; York, G.; Dwight, D. W.; McGrath, J. E.; Stejskal, J.; Kratochvil, P. *Polym. Prepr. (Am. Chem. Soc., Div. Polym. Chem.)* **1987**, *28* (1) 458.
- (15) Smith, S. D.; York, G.; Dwight, D. W.; McGrath, J. E. *Chemical Reactions on Polymers*; ACS Symposium Series No. 364; Benham, J. L., Kinstle, J. F. Eds.; American Chemical Society: Washington, DC, 1988; Chapter 7, pp 85-96.
- (16) DeSimone, J. M.; Hellstern, A. M.; Ward, T. C.; McGrath, J. E.; Smith, S. D.; Gallagher, P. M.; Krukoni, V. J.; Stejskal, J.; Strakova, D.; Kratochvil, P. *Polym. Prepr. (Am. Chem. Soc., Div. Polym. Chem.)* **1988**, *29* (2), 116.
- (17) DeSimone, J. M.; Hellstern, A. M.; Ward, T. C.; McGrath, J. E.; Smith, S. D.; Gallagher, P. M.; Krukoni, V. J. *Polym. Prepr. (Am. Chem. Soc., Div. Polym. Chem.)* **1988**, *29* (1), 361.



- (18) Hoover, J. M.; DeSimone, J. M.; Ward, T. C.; McGrath, J. E.; Smith, S. D. *Polym. Prepr. (Am. Chem. Soc., Div. Polym. Chem.)* **1988**, *29* (1), 166.
- (19) Smith, S. D.; DeSimone, J. M.; York, G.; Dwight, D. W.; Wilkes, G. L.; McGrath, J. E. *Polym. Prepr. (Am. Chem. Soc., Div. Polym. Chem.)* **1987**, *28*, (2), 150.
- (20) Kawakami, Y.; Murthy, R. A. N.; Yamashita, Y. *Makromol. Chem.* **1984**, *185*, 9.
- (21) Cameron, G. G.; Chisholm, M. S. *Polymer* **1985**, *26*, 437.
- (22) Kawakami, Y.; Yamashita, Y. *ACS Symp. Ser.* **1985**, No. 286, 245.
- (23) Saam, J. C.; Ward, A. H.; Fearon, F. W. G. *Polym. Prepr. (Am. Chem. Soc., Div. Polym. Chem.)* **1972**, *13* (1), 524.
- (24) Bostick, E. E. *Block Copolymers*; Aggarwal, S. L., Ed.; Plenum: New York, 1970; pp 237-247.
- (25) Kawakami, Y.; Miki, Y.; Tsuda, T.; Murthy, R. A. N.; Yamashita, Y. *Polym. J.* **1982**, *14* (11), 913.
- (26) Stejskal, J.; Strakova, D.; Kratochvil, P.; Smith, S. D.; McGrath, J. E. *Macromolecules* **1989**, *22* (2), 861.
- (27) DeSimone, J. M.; Hellstern, A. M.; Siochi, E. J.; Smith, S. D.; Ward, T. C.; Gallagher, P. M.; Krukoni, V. J.; McGrath, J. E. *Makromol. Chem., Macromol. Symp.* **1990**, *32*, 21.
- (28) Hashimoto, T.; Tsukahara, Y.; Tachi, K.; Kawai, H. *Macromolecules* **1983**, *16* (4), 648.
- (29) Alexander, L. E. *X-ray Diffraction Methods in Polymer Science*; Wiley: New York, 1969.
- (30) Patel, N. M.; Dwight, D. W.; Hedrick, J. L.; Webster, D. C.; McGrath, J. E. *Macromolecules* **1988**, *21* (9), 2689.

**Registry No.** (PDMS)(MMA) (copolymer), 110507-50-1.